

Evaluating Thermal Exposure Effects on Dielectric and Structural Properties of Water Treatment Residuals

M. A. H. Md Arfan¹, Z. I. Khan^{2*}, M. S. A. Megat Ali², S. A. E. Ab Rahim², Kamel Haddadi³, Zulfikri Suboh⁴

- ¹ College of Engineering,
Universiti Teknologi MARA (UiTM) Shah Alam, Shah Alam, 40450, MALAYSIA
- ² Microwave Research Institute (MRI),
Universiti Teknologi MARA (UiTM) Shah Alam, Shah Alam, 40450, MALAYSIA
- ³ Institute of Electronics, Microelectronics and Nanotechnology (IEMN),
University of Lille, Lille, FRANCE
- ⁴ Sungai Harmoni Sdn.Bhd,
Menara LGB, Kuala Lumpur, 40450, MALAYSIA

*Corresponding Author: zuhai629@uitm.edu.my

DOI: <https://doi.org/10.30880/ijie.2025.17.06.013>

Article Info

Received: 20 March 2025

Accepted: 17 October 2025

Available online: 30 December 2025

Keywords

Water treatment plant residuals (WTRs), microwave heating, dielectric permittivity, microwave non-destructive testing (MNNDT), morphological changes

Abstract

Effective handling of water treatment residuals (WTRs) is essential due to their substantial volume and environmental impact. This study investigates the effects of two thermal treatment methods—microwave and oven heating—on the dielectric properties and morphological changes of WTRs. Utilizing Microwave Non-Destructive Testing (MNNDT), dielectric permittivity was measured using a vector network analyzer, while morphological transformations were assessed through scanning electron microscopy (SEM). Microwave heating at power levels of 450W, 600W, and 800W resulted in a consistent increase in dielectric permittivity, ranging from 0.94 to 1.26, indicating improved dipolar alignment and material response. In contrast, oven heating produced less predictable results, with dielectric permittivity decreasing from 1.03 at 100°C to -0.55 at 200°C. SEM analysis further confirmed that microwave-treated samples exhibited more uniform structural modifications, including particle fusion and smoother surface morphology, compared to the more fragmented and heterogeneous changes observed under oven heating. The findings support the potential of microwave heating combined with MNNDT as a more effective and non-invasive method for characterizing and transforming WTRs. This approach could contribute to the development of more efficient and sustainable residual management processes in the water treatment industry.

1. Introduction

Water treatment residuals (WTRs) are byproducts generated during the purification process of potable water. These residuals, which contain a heterogeneous mix of organic and inorganic substances, are typically produced in large volumes and pose environmental concerns if not managed appropriately [1]. Conventional disposal practices, such as landfilling or reuse as soil conditioners, have been widely adopted. However, these methods often face limitations. Landfilling may result in leachate formation and potential groundwater contamination, while agricultural reuse can be hindered by the presence of heavy metals and other contaminants [2]- [4].

To address these limitations, there is a growing interest in developing alternative treatment and techniques that are environmentally sustainable and technically feasible. One emerging approach involves the evaluation of dielectric properties, particularly dielectric permittivity, which reflects a material's ability to store electrical energy when exposed to an electric field [5]. Understanding the dielectric behaviour of WTRs can provide insight into their internal structure, composition, and potential for further processing.

Microwave Non-Destructive Testing (MNNDT) has been identified as a promising technique for characterizing dielectric properties due to its rapid, contactless, and non-invasive nature [6]. When combined with thermal treatment, MNNDT enables real-time assessment of physical and dielectric changes in materials. Microwave heating has been reported to provide more efficient and uniform energy distribution than conventional oven heating, potentially leading to enhanced material transformation [7]. Conversely, oven heating typically results in slower, surface-driven thermal effects, which may produce less uniform structural modifications [8].

This study presents a comparative analysis of microwave and oven heating on the dielectric permittivity and morphological characteristics of WTRs. The objective is to evaluate the effectiveness of each heating method and to explore the application of MNNDT as a diagnostic tool for supporting sustainable residual management strategies.

2. Methodology

The following steps as shown in Fig. 1 outline the detailed experimental procedures designed to ensure consistency, accuracy, and reproducibility in the analysis of these residuals.

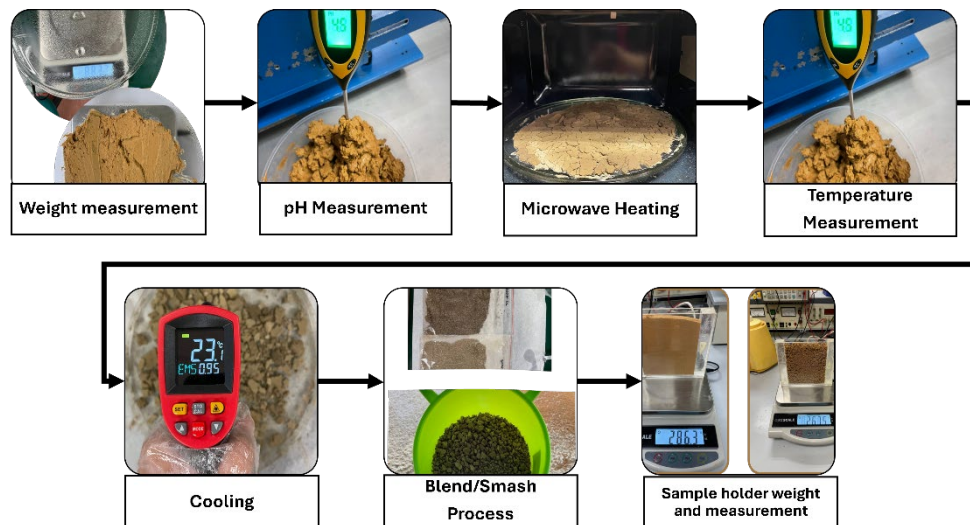


Fig. 1 Research methodology for WTRs heating process

2.1 Sample Preparation

WTR samples were collected and weighed using a precision balance to ensure uniform mass across all experimental conditions. The pH of each sample was also measured with a digital pH meter to establish a baseline for chemical behaviour during heating. This step ensured consistency in both physical and chemical parameters prior to thermal exposure. By knowing the starting pH, researchers can detect shifts in acidity or alkalinity that resulted from microwave or oven heating, which can affect the material's properties and behaviour [11]. Such changes in pH can influence the dielectric properties and structural integrity of the WTRs, making it an important parameter to monitor.

2.2 Thermal Treatment

2.2.1 Microwave Heating and Oven Heating

In this experimental study, a laboratory-grade microwave oven with adjustable power settings was employed to thermally treat the water treatment residual (WTR) samples. To maintain material integrity, all samples were placed in microwave-compatible containers designed to withstand electromagnetic exposure. Heating was conducted at three distinct power levels—450W, 600W, and 800W—based on the operational capacity of the equipment. These power settings were selected to examine the influence of varying energy inputs on the dielectric

behavior of the samples. Heating durations were carefully calibrated for each power level to achieve consistent thermal exposure, thereby minimizing the risks of overheating or insufficient treatment. This controlled variation in both power and duration was intended to identify optimal conditions for enhancing dielectric properties without compromising the structural characteristics of the material [12].

In parallel, oven heating was performed using a conventional laboratory oven set to three fixed temperatures: 100°C, 150°C, and 200°C. Each sample was placed in a ceramic crucible and subjected to uniform heating for a predetermined duration to ensure thermal equilibrium throughout the sample mass. Oven temperatures were chosen to simulate gradual conductive heat transfer, providing a contrast to the rapid volumetric heating observed in microwave exposure. This slower heating process is known to induce surface-dominant changes and can potentially result in thermal gradients that affect the material's internal structure. By comparing results from these two methods, the study aimed to capture the nuances of energy delivery mechanisms—volumetric dielectric heating versus surface conduction—and their influence on WTR transformation.

Together, these thermal protocols provided a comprehensive understanding of how heating intensity and modality affect the dielectric and microstructural properties of WTRs, with implications for improving their reuse and treatment pathways.

2.2.2 Cooling Process

Following microwave treatment, the WTR samples were allowed to cool naturally to room temperature prior to any further analysis. This cooling phase is essential to stabilize the dielectric response, as residual thermal excitation and molecular dipole reorientation can lead to transient fluctuations in permittivity. Allowing the material to return to ambient conditions also helps preserve its structural integrity by reducing thermal stresses that might otherwise result in microcracking or deformation [13]. Moreover, standardizing the temperature of all samples before measurement ensures safe handling and improves experimental reproducibility. This step adheres to established practices in material characterization, ensuring that any changes in the samples' dielectric or morphological properties are directly attributable to the heating process and not influenced by uncontrolled thermal variables.

2.2.3 Sample Homogenization and Mass Verification

After cooling, the samples were mechanically blended to achieve uniform composition and texture. This homogenization process is essential for ensuring consistent results during dielectric and morphological evaluations. Samples were then reweighed together with the dielectric sample holders to maintain mass accuracy during measurement.

2.3 Microwave Non-Destructive Testing (MNDT)

Microwave non-destructive testing (MNDT) is an ideal method for measuring dielectric properties at microwave frequencies in this investigation [14]. The process is contactless, has good penetration of nonmetallic materials, and does not need sample machining for exact fitting, as other methods do, MNDT's major components are a pair of horn lens antennas, a network analyzer, and a sample holder as depicted in Figure 2. A pair of identical Plano-convex dielectric lens antennas provide the required antenna for spot focusing on the setup. In free space measurements, a spot-focusing antenna is used to eliminate errors caused by diffraction effects at the material's edges and numerous reflections. The horn antennas are connected to the vector network analyzer by means of a pair of coaxial cables, as well as rectangular-to-circular and coaxial-to-rectangular waveguide adapters. Two Perspex plates hold the sample in place between the two antennas [15][16].

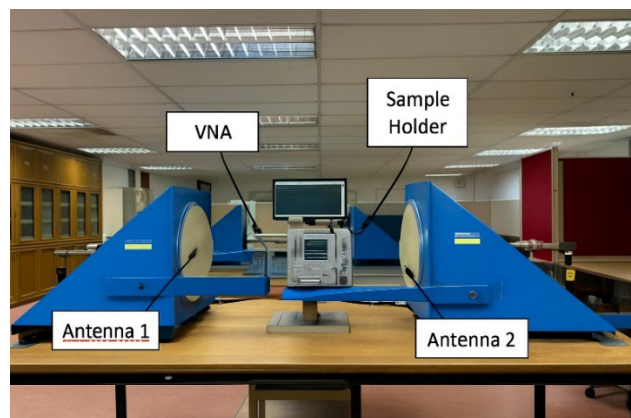


Fig. 2 Free space MNDT (X-Band) laboratory setup

The S-parameters data were extracted from the free space measurement system using the VNA and MATLAB coding was used to display the response graph of S_{11} and S_{21} in terms of real and imaginary values versus X-band frequency (8 GHz to 12 GHz) for S_{11} and S_{21} . This process allows for the visualization of the complex behaviour of the S-parameters over the X-band frequency range, providing insights into the dielectric properties of the samples. The response graph of S_{11} and S_{21} helps in understanding how the samples interact with the electromagnetic fields at different frequencies, which is essential for characterizing the material's composition, moisture content, and structural integrity [17][18].

2.4 Dielectric Permittivity Measurement and Morphological Analysis

The dielectric permittivity of each sample was determined by analyzing the S-parameter responses obtained through Microwave Non-Destructive Testing. To ensure measurement reliability, each sample was tested three times, and the average value was used for subsequent analysis. These permittivity values were then evaluated to identify trends and variations resulting from the different thermal treatments, microwave and oven heating. For the morphological assessment, representative portions of each sample were prepared and mounted onto Scanning Electron Microscope (SEM) stubs. Micrographs were acquired at multiple magnifications to capture detailed structural features. Quantitative analysis of the SEM images was performed using image processing software to evaluate parameters such as pore size, spatial distribution, and surface roughness, enabling a comparative interpretation of microstructural changes induced by each heating method.

2.5 Data Analysis

This methodology establishes a structured and repeatable approach for evaluating how microwave heating influences the dielectric permittivity and microstructural attributes of water treatment residuals (WTRs). The comprehensive procedural steps outlined in this study are designed to ensure experimental consistency and facilitate result validation. To support a deeper understanding of the observed changes in dielectric and morphological behavior following both microwave and oven heating, it is important to consider the fundamental mechanisms through which thermal energy interacts with the material.

Microwave heating is believed to enhance polarization mechanisms within WTRs more effectively than conventional heating, particularly by promoting dipolar alignment and ionic mobility, which may account for the observed increase in dielectric permittivity [19]. Moreover, morphological modifications—such as increased porosity and expanded surface area, as evident from SEM analysis—can influence dielectric properties by altering bulk density and interfacial polarization effects, commonly described by the Maxwell-Wagner-Sillars phenomenon [15]. These thermally induced changes can be theoretically interpreted using classical dielectric models, such as the Debye relaxation model and the Clausius-Mossotti relation, which offer predictive insights into the relationship between microstructure and dielectric response [20].

Based on our analysis of the raw residuals, there were no significant initial differences between Sample 1 and Sample 5. The S-parameter plots depicting the raw residual demonstrate a consistent frequency domain response across all 5 samples taken. It indicates that our experimental setup and methodology provide reliable and repeatable measurements of these critical dielectric properties. This means that the differences or similarities we observe between samples are truly due to their intrinsic material properties and the effects of the microwave treatment, rather than measurement inconsistencies.

This ability to consistently characterize the dielectric properties of these residuals, even after microwave heating at different power levels, is a significant step forward. It allows us to better understand how water treatment sludge reacts to microwave energy, which is foundational for optimizing processes like dewatering and drying. The S-parameter plots for the raw residuals were also consistent across all five samples that were subjected to oven heating. This confirms that our experimental setup and methodology were reliable for measuring the dielectric properties, irrespective of the heating method used. Therefore, any observed differences in the S-parameter plots of the oven-heated samples can be confidently attributed to the effects of the thermal treatment itself and not to initial inconsistencies in the samples.

3. Results and Discussion

3.1 Microwave Heating on the S-Parameter Response

The resonance effects observed in the S_{11} plot display how the microwave heating altered the dielectric properties of the dust samples as shown in Fig. 3, Fig. 4 and Fig. 5. The variations in S_{11} and S_{21} amplitudes among the samples also imply that microwave heating may have altered the dielectric properties to different degrees, possibly due to the variations in density or composition of the samples. An increasing trend in dielectric losses at higher frequencies, which might have been impacted by the microwave heating process could be the reason for the decreasing trend in S_{21} amplitudes with increasing frequency.

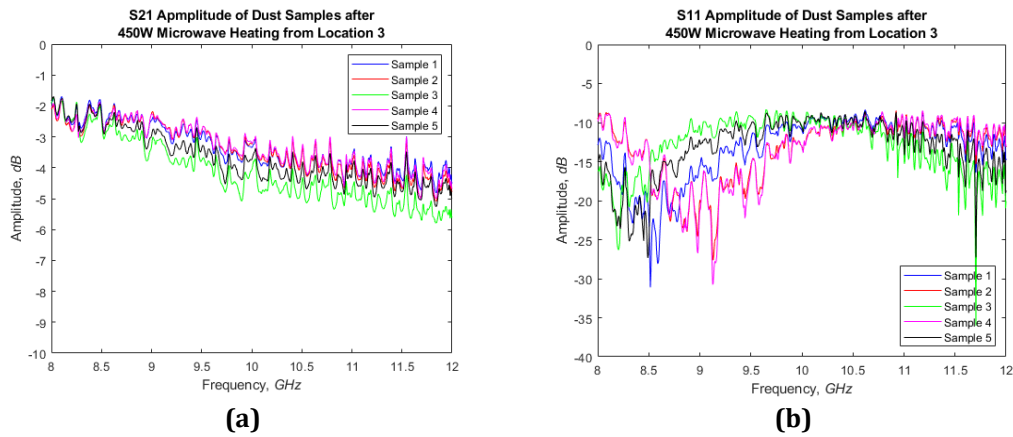


Fig. 3 Frequency response of S_{11} and S_{21} of dust samples at 450 W (a) S_{21} amplitude; (b) S_{11} amplitude

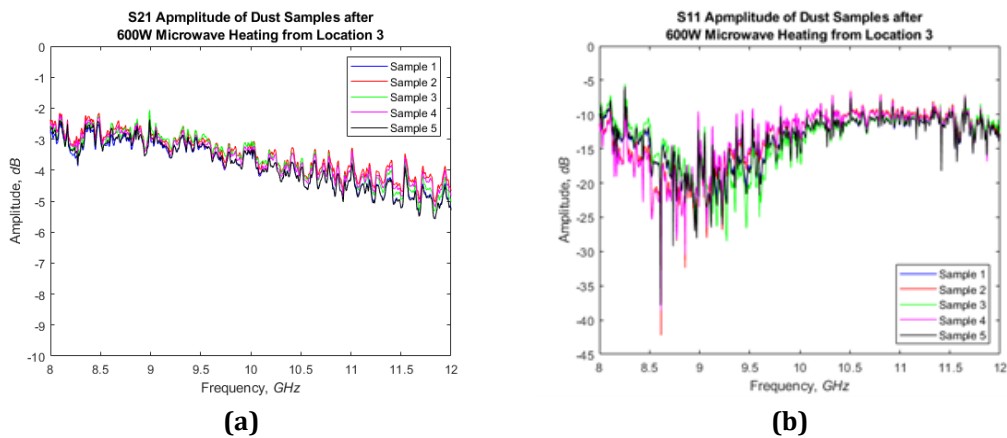


Fig. 4 Frequency response of S_{11} and S_{21} of dust samples at 600 W (a) S_{21} amplitude; (b) S_{11} amplitude

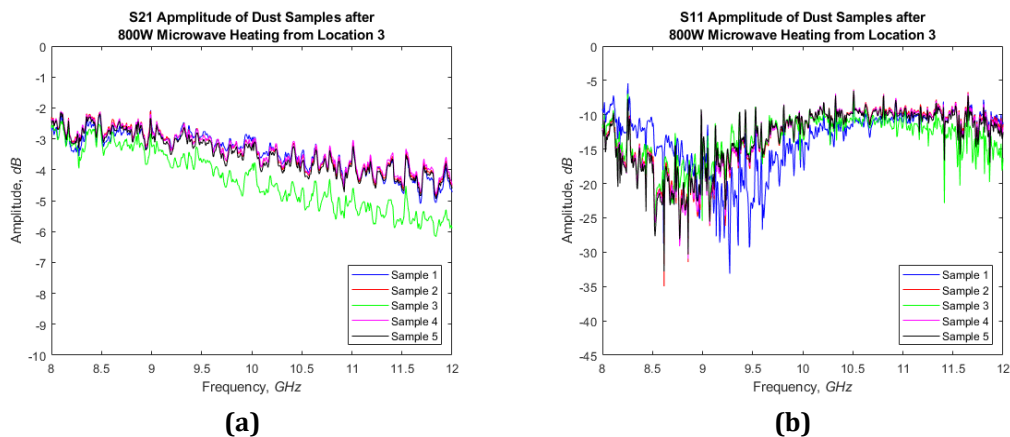


Fig. 5 Frequency response of S_{11} and S_{21} of dust samples at 800 W (a) S_{21} amplitude; (b) S_{11} amplitude

The overall fluctuations and variations in the S-parameter magnitudes indicate that the dielectric properties of the dust samples have been modified by microwave heating which has an impact on how the dust samples interact with electromagnetic waves in the microwave frequency range. The S-parameter amplitude changes that were observed reveal how sensitive the microwave non-destructive testing (MNDT) is in identifying dielectric property variations resulting from different microwave heating power levels.

3.2 Oven Heating on S-Parameter Response

Looking at the S_{21} plot, most samples fall between -2 and -3 dB, with sample 4 (green) standing out slightly which allows more signal through, hovering closer to -1.5 dB. This indicates sample 4 is just a bit less resistive to signal transmission than the rest as shown in Fig. 6(a). While on Fig. 6(b), the S_{11} plot depicts a familiar picture with sharp dips between frequency of 9 and 10 GHz, especially for samples 4 and 5. Those dips reach nearly -50 dB which show strong absorption at those frequencies. The rest of the range stays relatively smooth, indicating decent absorption overall. Overall, at 150 °C, the dust samples are mostly uniform, but sample 4 stands out with slightly better transmission and deeper absorption dips, pointing to minor variations in how it responds to microwave frequencies.

The S_{21} plot in Fig. 7(a) shows all five samples follow almost the same path. Their amplitude gradually drops from around -2 dB to about -3.5 dB as frequency increases. This indicates that the material slightly loses more signal at higher frequencies, but overall, all samples behave similarly suggesting they responded uniformly to the heating. The S_{11} plot in Fig. 7(b), also reveals tight groupings. There is a strong dip between frequency of 9 and 10 GHz, hitting as low as -50 dB in a couple of samples, which indicates a great absorption of the signal at that range. That deep dip stands out, but otherwise, the reflection stays between -10 and -20 dB which is a good balance.

In the S_{21} plot as shown in Fig. 8(a), all five lines closely track each other, staying mostly between -2 and -3.5 dB. Sample 4 (purple) is slightly higher in amplitude at some points which indicates it let a bit more signal pass through than the rest which could be due to a subtle change in its makeup after the heating. While in the S_{11} plot as shown in Fig. 8(b), there are some deep dips again especially around 10 GHz, where some samples drop below -50 dB. That suggest the samples are doing a solid job absorbing signal in that range. The rest of the frequencies stay uniform, between -10 and -20 dB.

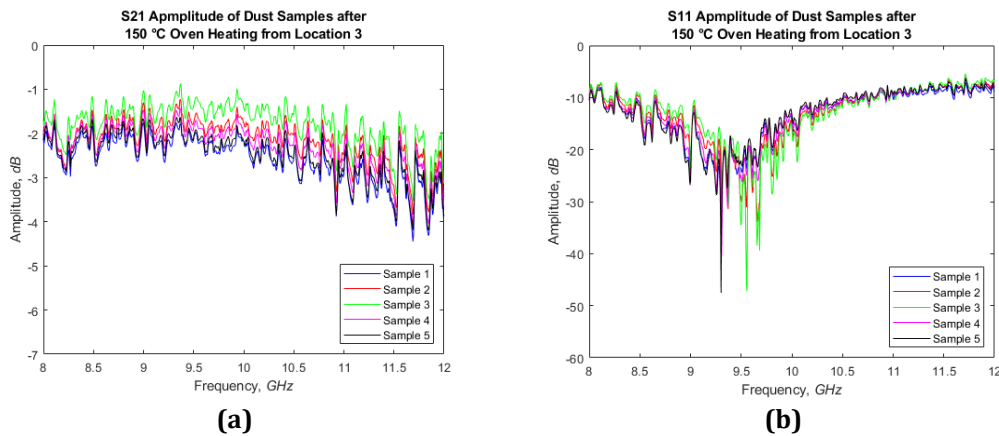


Fig. 6 Frequency response of S_{11} and S_{21} of dust samples at 150°C (a) S_{21} amplitude; (b) S_{11} amplitude

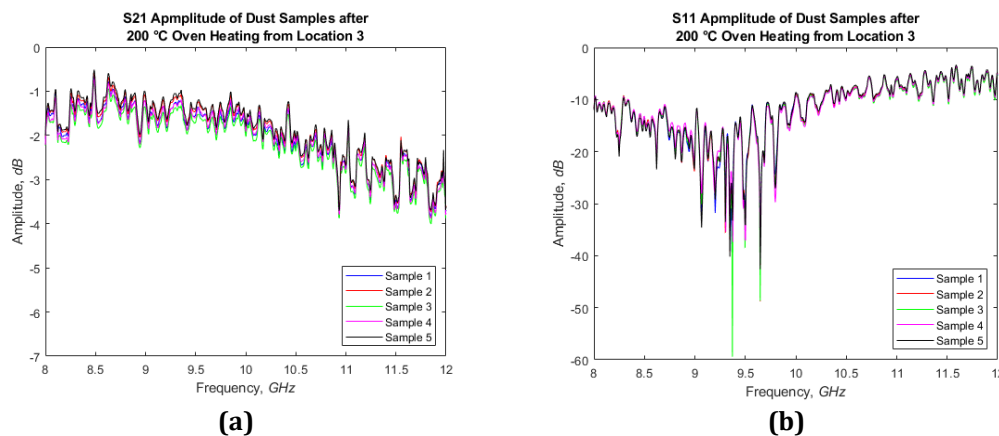


Fig. 7 Frequency response of S_{11} and S_{21} of dust samples at 200°C (a) S_{21} amplitude; (b) S_{11} amplitude

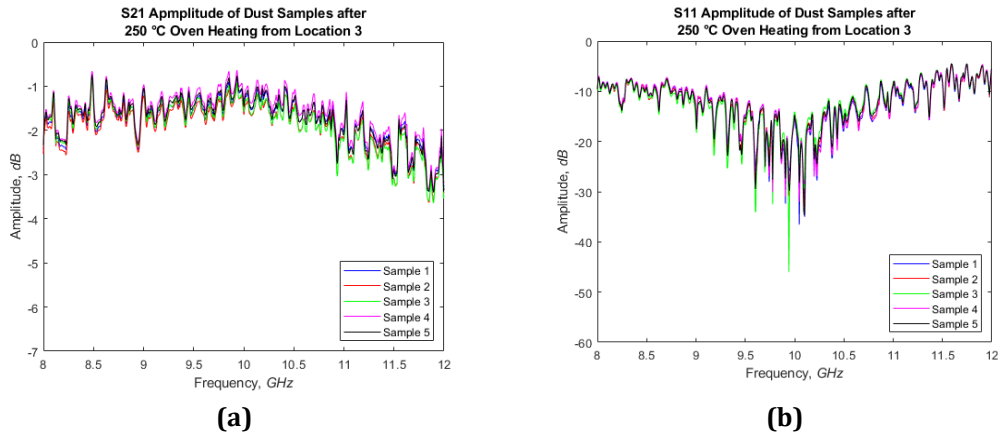


Fig. 8 Frequency response of S_{11} and S_{21} of dust samples at 200°C (a) S_{21} amplitude; (b) S_{11} amplitude

3.3 Dielectric Permittivity of Microwave and Oven-Heated Residuals

Detailed analysis of SEM images was integrated with dielectric permittivity measurements to provide deeper insights into how structural changes at the microscopic level influence material properties. The SEM images were taken with two values of magnifications: 10 μm and 5 μm . Microwave heating demonstrated a clear trend where increasing power levels from 450W to 800W resulted in progressively higher dielectric permittivity values. This increase suggests that microwave energy enhances the alignment of molecular dipoles, which in turn facilitates a greater capacity to store electrical energy. The following is the recorded dielectric permittivity measurement of the microwave and oven-heated samples.

Table 1 The recorded measurements of the microwave-heated samples

| Microwave Heating Power (W) | Sample | Heating durations (minutes) | Weight (g) | | Temperature ($^{\circ}\text{C}$) | | Dielectric Permittivity (DP) |
|-----------------------------|--------|-----------------------------|------------|-------|------------------------------------|-------|------------------------------|
| | | | Before | After | Before | After | |
| 450 | 1 | 30 | 500 | 300.2 | 29 | 63 | 2.9 |
| | 2 | | | 305.2 | 28 | 72 | 3.3 |
| | 3 | | | 305.9 | 28 | 68 | 4.1 |
| | 4 | | | 303.5 | 25 | 74 | 4.4 |
| | 5 | | | 306.2 | 25 | 74 | 4.5 |
| 600 | 1 | 20 | 500 | 323.3 | 24 | 59 | 1.0 |
| | 2 | | | 318.7 | 22 | 49 | 3.2 |
| | 3 | | | 324.1 | 24 | 59 | 3.1 |
| | 4 | | | 329.2 | 23 | 49 | 1.4 |
| | 5 | | | 324.8 | 21 | 59 | 2.1 |

| Microwave Heating Power (W) | Sample | Heating durations (minutes) | Weight (g) | | Temperature (°C) | | Dielectric Permittivity (DP) |
|-----------------------------|--------|-----------------------------|------------|-------|------------------|-------|------------------------------|
| | | | Before | After | Before | After | |
| 800 | 1 | 16 | 500 | 320.2 | 24 | 59 | 3.1 |
| | 2 | | | 314.2 | 24 | 61 | 3.5 |
| | 3 | | | 304.7 | 23 | 51 | 3.6 |
| | 4 | | | 323.5 | 25 | 62 | 1.2 |
| | 5 | | | 316.3 | 21 | 53 | 3.7 |

Table 2 The recorded measurements of the oven-heated samples

| Oven Temperature (°C) | Sample | Heating durations (minutes) | Weight (g) | | Temperature (°C) | | Dielectric Permittivity (DP) |
|-----------------------|--------|-----------------------------|------------|-------|------------------|-------|------------------------------|
| | | | Before | After | Before | After | |
| 100 | 1 | 180 | 500 | 283.9 | 21 | 63 | -0.4 |
| | 2 | | | 285.7 | 20 | 55 | 0.5 |
| | 3 | | | 292.7 | 22 | 53 | 0.8 |
| | 4 | | | 299.5 | 23 | 54 | 1.0 |
| | 5 | | | 291.7 | 24 | 55 | 0.7 |
| 150 | 1 | 110 | 500 | 276.6 | 24 | 57 | 3.8 |
| | 2 | | | 267.9 | 21 | 62 | 1.6 |
| | 3 | | | 277.5 | 21 | 60 | 1.2 |
| | 4 | | | 274.5 | 22 | 55 | 1.5 |
| | 5 | | | 271.4 | 22 | 60 | 1.2 |
| 200 | 1 | 70 | 500 | 265.5 | 23 | 70 | 1.1 |
| | 2 | | | 261.7 | 22 | 72 | 1.2 |
| | 3 | | | 266.3 | 22 | 67 | 1.1 |
| | 4 | | | 264.7 | 21 | 67 | 1.1 |
| | 5 | | | 268.2 | 23 | 63 | 1.1 |

3.4 Molecular Structure of Microwave and Oven-Heated Residuals (SEM)

The SEM or scanning electron microscope is used in this part to provide insights into the molecular structure of the sample which is the dried residuals that have undergone microwave heating at different power levels. The SEM enables the observation of the surface methodology and topography of the dust particles at high magnification. It may appear in different particle sizes, shapes, agglomeration, and surface textures between the samples heated. Figs. 9 to 14 refers to the five samples (Samples 1 to 5) that underwent thermal treatment. The specific samples are not individually labeled in the figures because the S-parameter plots for the raw residuals demonstrated a consistent frequency domain response across all five samples. This indicates that their initial intrinsic material properties were consistent, and therefore, the differences observed in the treated samples are a direct result of the microwave or oven heating process.

3.4.1 At Power of 450 Watt

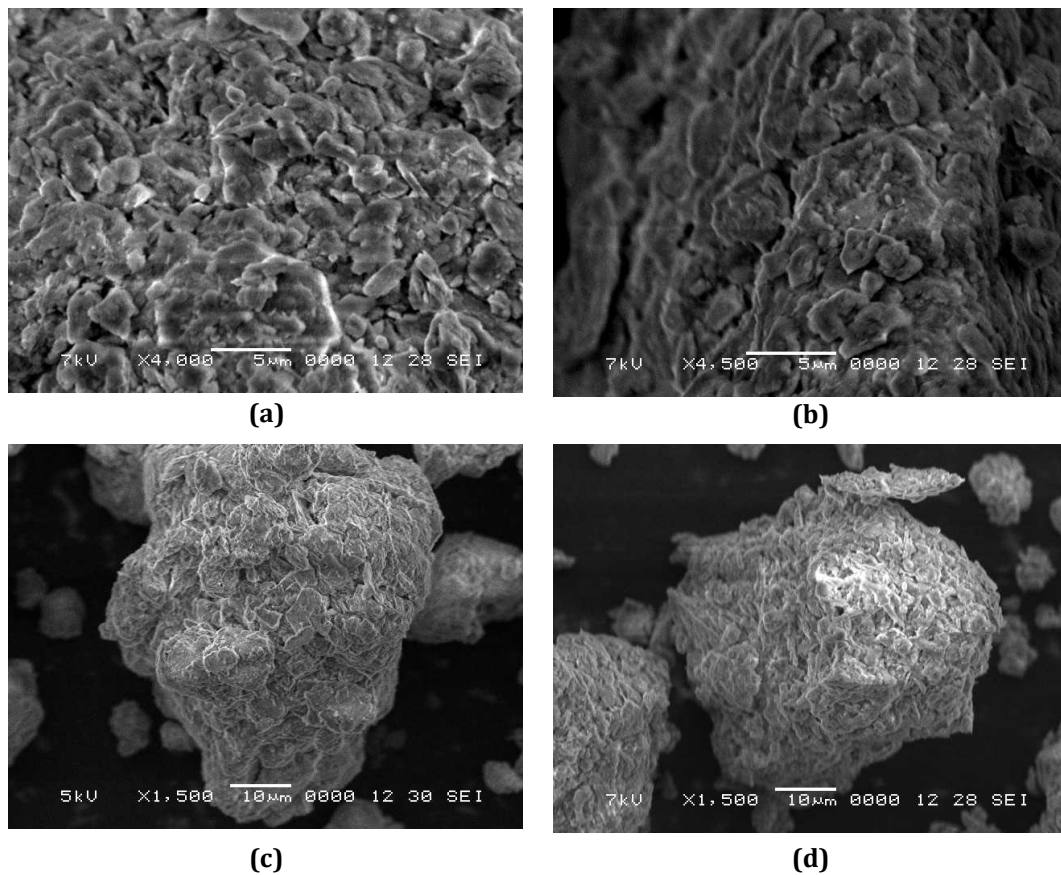


Fig. 9 Molecular structure of dried sludge at 450 W (a) 5μ at 4k magnification; (b) 5μ at 4.5k magnification; (c) 10μ at 1.5k magnification; (d) 10μ at 1.5k magnification

Fig. 9 depicts a highly porous and irregular structure with many voids and cavities of different sizes at different magnifications. This implies that a highly porous material with a sizable surface area has been formed resulting from the 450-watt microwave heating process. It reveals that the dried residual particles have agglomerated and formed larger, irregularly shaped aggregates. It appears that the smaller, irregularly shaped particles that make up these aggregates have merged or stuck to one another during the heating process.

Both the aggregates and the individual particles' surfaces have many extensions and irregularities which gives them a textured and rough appearance [21]. This surface roughness and texture can be attributed to the thermal effects of microwave heating which may have prompted molecular rearrangements, melting, or degradation of the organic components within the sludge material [22]. The dark contrast observed in the images indicates the presence of carbonized or charred organic material [23]. High-temperature microwave heating can cause organic compounds to decompose and become carbonized which creates structures that are rich in carbon [24].

Such a tortuous, high surface area structure is typical of activated carbons produced from carbon-rich precursors like coal, coconut shells, or biomass that have undergone thermal activation processes involving controlled oxidation or chemical treatment [25]. The activation process burns off some of the disordered

carbonaceous material, leaving behind a highly porous solid riddled with gaps and crevices. The random, contorted shapes and the significant porosity visible in this SEM image strongly resemble the microstructures commonly seen in activated carbon samples examined under electron microscopy [26]. The morphology is consistent with the highly convoluted pore network that gives activated carbons their exceptional surface area for adsorption applications [27].

3.4.2 At Power of 600 Watt

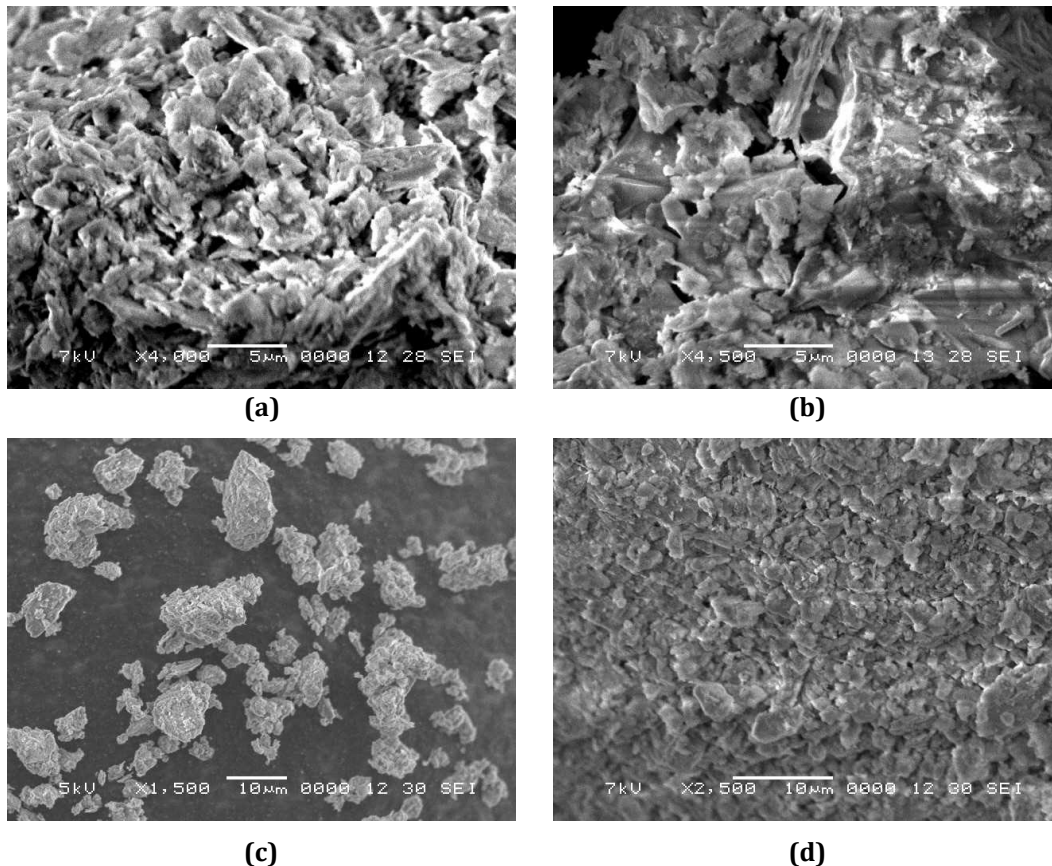


Fig. 10 Molecular structure of dried sludge at 600 W (a) 5 μ at 4k magnification; (b) 5 μ at 4.5k magnification; (c) 10 μ at 1.5k magnification; (d) 10 μ at 2.5k magnification

From Fig. 10, the micrographs depict the surface structure of dried sludge in four different magnifications. The particles appear to be merged or clustered together which have an irregular, rough surface topography with cracks, pores, and extensions visible. The overall structure indicates a solid material that has undergone some thermal processing which is microwave heating which results in a non-uniform granular microstructure [28]. The plate-like features appear more disorganized, fragmented, and jagged compared to the smoother, more graphitic platelets often seen in activated carbons [29]. The overall structure seems more chaotic, with a less well-defined pore architecture than the more ordered, maze-like channels found in many activated carbons [30].

There appears to be a wider range of pore sizes, including some larger cavities that may indicate partial melting or sintering of the material at the higher heating temperature (600 Watts) [31]. These changes could have included phase transitions, dehydration, or the formation of new crystalline phases like mullite, cristobalite, or illite as observed in [32].

The heating process most likely caused changes in the molecular structure of the clay. Heat causes specific transformations in clay minerals that are indicative of their mineralogical composition, including the creation of new phases and modifications to their crystal structure [33]. However, water treatment plant residuals might not undergo the same mineralogical changes when heated as clays due to the significant differences in their composition. The residuals may not exhibit similar mineralogical transformations but the clay samples probably will display changes related to their mineral content under the same heating conditions [34].

3.4.3 At Power of 800 Watt

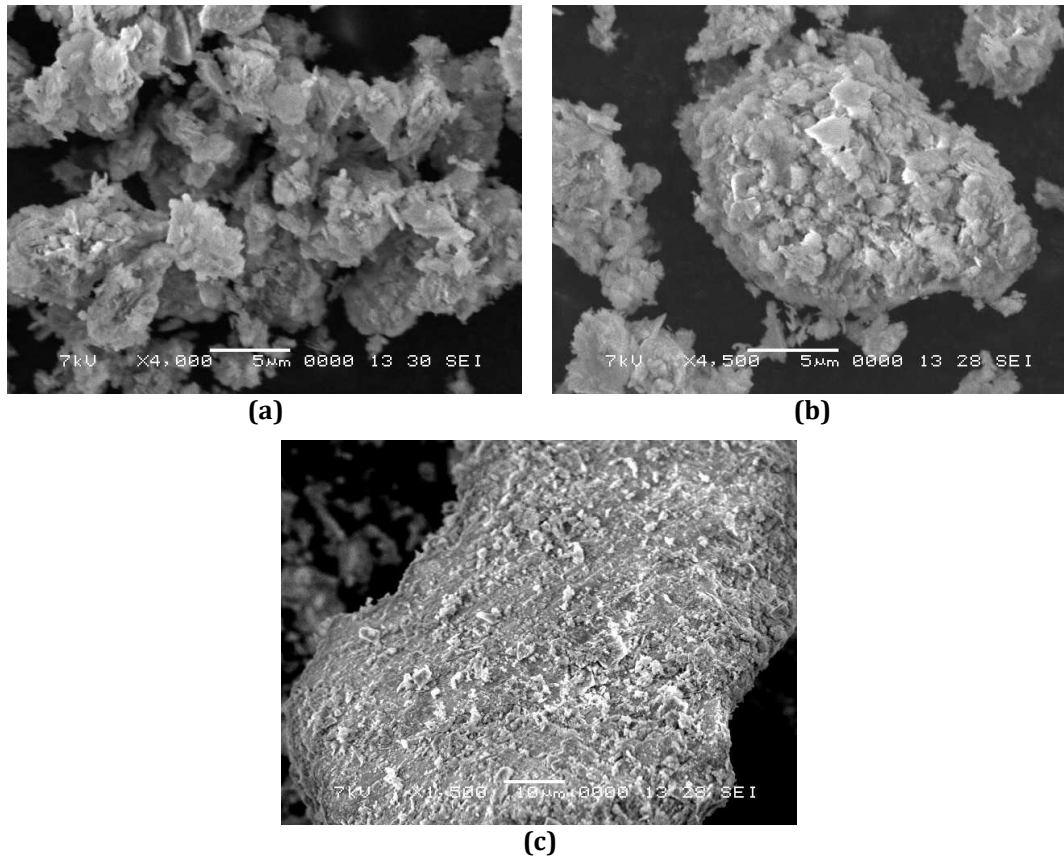


Fig. 11 Molecular structure of dried sludge at 800 W (a) 5 μ at 4k magnification; (b) 5 μ at 4.5k magnification; (c) 10 μ at 1.5k magnification

Based on Fig. 11, irregular texture is observed, the samples also appear to have a polycrystalline or amorphous microstructure composed of small grains or particles aggregated together. The different shades of grey indicate differences in the surface topography, with brighter regions that are pointing in the direction of the electron beam and darker regions indicating cavities or depressions. During the heating process, both heated soil and heated water treatment plant residuals undergo dehydration where water molecules are removed from the material's structure which leads to alterations in the crystal lattice structure and rearrangement of atoms.

Compared to soil samples, heated water treatment plant residuals may display more noticeable changes in particle size and aggregation due to the presence of organic matter and chemical interactions. The chemicals used in the water treatment process such as coagulants (like alum and ferric salts) and softeners (like lime) may be more concentrated in water treatment plant residuals. This could have an impact on the molecular structure and behaviour of the residuals during heating [35].

While some residual porosity may be present, the overall microstructures in these two SEM micrographs do not exhibit the characteristic features of pristine, well-developed activated carbon materials, such as: ordered arrays of graphitic platelets, interconnected networks of uniform micropores and mesopores and high surface area due to extensive internal porosity. Instead, the observed morphologies appear to be the result of severe thermal treatment, potentially leading to the collapse or melting of any initial porous structure and the formation of irregularly shaped, sintered-like particles with limited accessible porosity. It is unlikely that these SEM images represent the microstructure of a typical activated carbon material based on the observed morphological features [36].

3.4.4 At Temperature of 100°C

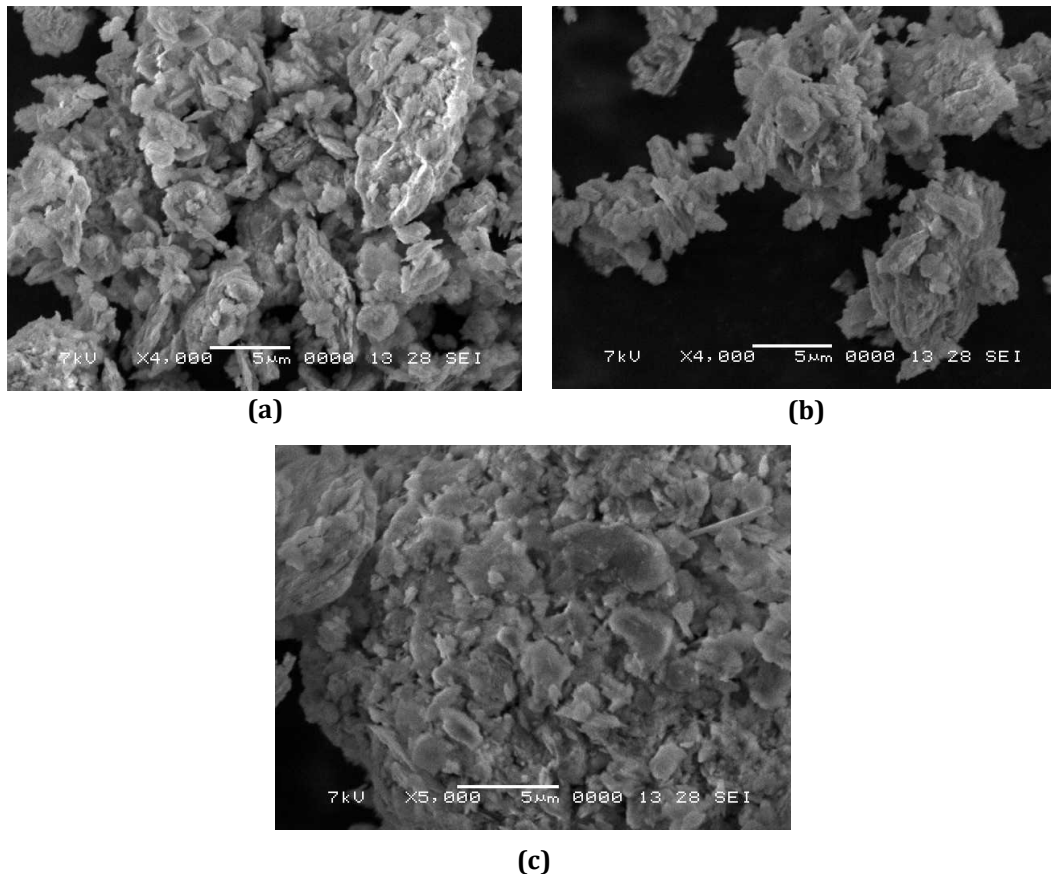


Fig. 12 Molecular structure of dried sludge at temperature of 100°C (a) 5µ at 4k magnification; (b) 5µ at 4k magnification; (c) 5µ at 5k magnification

Fig. 12 depicts the dried sludge retains a slightly cohesive but less compact structure at 100°C in contrast to higher temperature treatments. The particles have loosely associated clusters and a flake-like structure with comparatively soft edges. Although the general texture is rough, it does not exhibit the noticeable rigidity or fragmentation that is observed at higher temperatures, indicating that the sludge's structural integrity is mostly maintained at this temperature.

In addition, the sludge particles appear to retain some degree of moisture and flexibility, resulting in a more aggregated and less brittle arrangement. There are surface characteristics, but they are not as distinct, suggesting that the drying process is more slow and less disruptive to the interior bonding of the material at this temperature.

Furthermore, although there are some early indications of porosity and layering in the material, the structural evolution is still quite faint. This degree of heat treatment appears to be adequate to remove surface moisture and encourage slight aggregation without significantly changing the internal structure of the sludge or promoting micro fracturing

In conclusion, sludge dried at 100°C exhibits preliminary morphological modifications that prepare the way for more significant structural changes at higher temperatures. It is appropriate for applications where little thermal change is desired because it strikes a compromise between dehydration and maintaining the native particle organisation.

3.4.5 At Temperature of 150°C

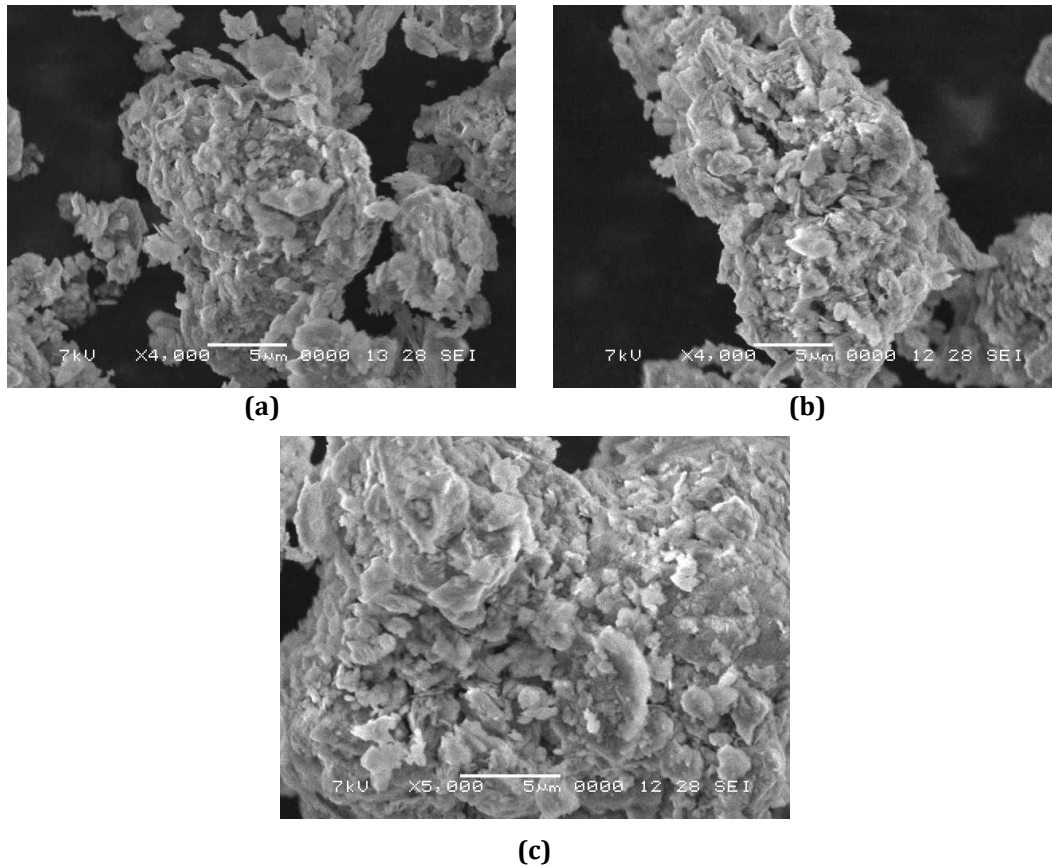


Fig. 13 Molecular structure of dried sludge at temperature of 150°C (a) 5µ at 4k magnification; (b) 5µ at 4k magnification; (c) 5µ at 5k magnification

From Fig. 13, the microstructure of the dried sludge changes noticeably at 150°C in contrast to lower temperature treatments. There are indications of increasing particle fusion and surface roughness, and the overall morphology becomes denser and more layered. According to these features, the higher temperature encourages more moisture loss and thermal contact between the particles, which results in partial shattering and a more rigid structure.

In addition, the surface texture appears more distinct and rougher, most likely due to the increased fragility and micro fracturing caused on by heat stress. This results in a more complex and porous surface, which may be advantageous for uses where pore accessibility and surface area are crucial, like adsorption or filtering.

Furthermore, a certain amount of fragmentation and brittle can be seen at lower magnifications, particularly in larger sample quantities, even though specific compaction is still noticeable. This suggests that while the heat treatment consolidates some areas, it also promotes particle separation and structural breakdown in other areas. This impact demonstrates the complex relationship between fragility and cohesiveness that develops with temperatures.

Overall, the sludge treated at 150°C changes into a more structurally differentiated and texturally complex material, which, depending on the intended end use, may improve its functional performance.

3.4.6 At Temperature of 200°C

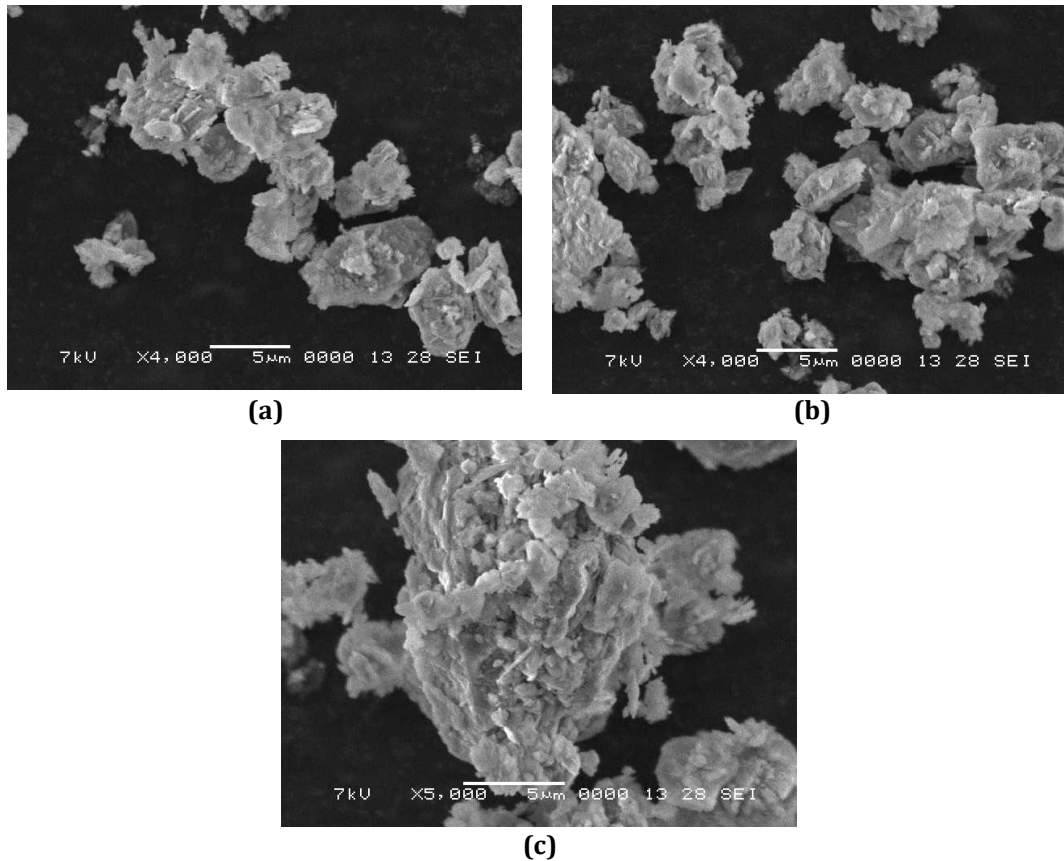


Fig. 14 Molecular structure of dried sludge at temperature of 200°C (a) 5µ at 4k magnification; (b) 5µ at 4k magnification; (c) 5µ at 5k magnification

Based on Fig. 14, the material becomes more brittle and fractured, as shown in the micrographs, with many of the former coherent clusters dissolving into smaller, more defined particles. This indicates that the sludge has progressed to a point where the particle integrity is being substantially changed by heat breakdown and the loss of volatile components.

Sharper edges and more pronounced particle boundaries define the overall morphology, which is characterised by flaky, sheet-like structures. Due to the heat breakdown of organic materials and subsequent rearranging of mineral components, these features show a change towards a more crystalline or layered appearance.

In addition, the particle dispersion seems to be more extensive, particularly in larger sample sizes at this temperature. There are more isolated pieces visible throughout the field of vision, indicating a less compact structure. This extensive disintegration suggests that the material has experienced enough heat stress to break down inter-particle cohesiveness, resulting in a highly porous and fragmented structure.

In conclusion, the sludge exhibits a significantly altered morphology which are fractured, more porous, and texturally complex after been oven-heated at 200°C. These properties point to possible benefits for uses like adsorption or as a precursor for carbon-based materials, where more surface area and structural flexibility are advantageous.

Overall, increasing microwave power leads to more uniform structural modification of the sludge, resulting in a more porous and irregular structure. The formation seen in Fig. 9 is similar to activated carbons, which is desirable for applications like adsorption. This structural change is attributed to the fast and volumetric heating of the microwave process, which creates internal pressure that leads to the formation of pores. In contrast, oven heating results in more compacted and less porous structures as temperature increases, with the formation of lumps and aggregates.

The results suggests that microwave heating is the best formation due to its more uniform structure with a higher porosity and surface area, which is beneficial for adsorption and other applications. The microwave-treated sludge also showed a consistent increase in dielectric permittivity, unlike the oven-treated samples.

4. Conclusion

This study has demonstrated that the choice of heating method significantly influences the dielectric and morphological characteristics of water treatment residuals (WTRs). Microwave heating produced more consistent enhancements in dielectric permittivity compared to conventional oven heating, which exhibited irregular trends and, at higher temperatures, even negative permittivity values. These outcomes suggest that microwave energy promotes more efficient dipolar alignment and internal structural reorganization due to its rapid and uniform heating profile. Morphological analysis using SEM further supported these findings, revealing that microwave-treated samples exhibited smoother surfaces and greater particle cohesion, while oven-treated samples showed more fragmented and heterogeneous structures, particularly at elevated temperatures. The integration of Microwave Non-Destructive Testing (MNDT) in this context proved to be a reliable approach for capturing real-time dielectric behavior, offering potential as a diagnostic tool for material evaluation and processing control. Overall, the results underscore the viability of microwave-based treatment as a more effective and sustainable method for managing WTRs. Future work should focus on optimizing heating parameters for large-scale applications, assessing the long-term stability of treated residuals, and evaluating their suitability for valorization pathways such as adsorption media or precursor materials in environmental engineering. Additional studies involving life cycle analysis and advanced material modeling could further refine the applicability of this technique within circular water management systems.

Acknowledgement

This research is funded and supported by Ministry of Higher Education (MOHE) through Fundamental Research Grant Scheme (FRGS) (FRGS/1/2023/TK08/UITM/02/8) and Microwave Research Institute UiTM, Shah Alam Selangor.

Author Contribution

*The authors confirm contribution to the paper as follows: **study conception and design:** Author 1, Author 2, Author 3, Author 4; **data collection:** Author 1, Author 4; **analysis and interpretation of results:** Author 3, Author 4, Author 5 ; **draft manuscript preparation:** Author 1, Author 2; **industrial collaboration:** Author 6; **technical and measurement validation:** Author 6. All authors reviewed the results and approved the final version of the manuscript.*

References

- [1] S. K. Sharma and M. M. Ahammed, "Sustainable management of water treatment residuals: Challenges and opportunities," *Journal of Environmental Management*, vol. 320, p. 116789, 2023.
- [2] J. A. Ippolito, K. A. Barbarick, and H. A. Elliott, "Drinking water treatment residuals: A review of recent uses," *Journal of Environmental Quality*, vol. 40, no. 1, pp. 1–12, 2011.
- [3] R. A. Barbosa, R. F. Gonçalves, and C. E. Teixeira, "Environmental and economic assessment of disposal of water treatment sludge in landfills," *Journal of Environmental Management*, vol. 229, pp. 173-183, 2019.
- [4] M. Zhang and X. He, "Heavy metal risks of municipal water treatment residuals used in agriculture: A review," *Environmental Science and Pollution Research*, vol. 27, pp. 4120-4132, 2020.
- [5] A. Von Hippel, *Dielectric materials and applications*, Artech House, 1995.
- [6] E. Nyfors, "Industrial microwave sensors—A review," *Subsurface Sensing Technologies and Applications*, vol. 1, no. 1, pp. 23–43, 2000.
- [7] A. C. Metaxas and R. J. Meredith, *Industrial microwave heating*, IET, 1983.
- [8] H. Zhang and A. K. Datta, "Microwave power absorption in single-and multiple-item foods," *Food and Bioproducts Processing*, vol. 78, no. 4, pp. 169–179, 2000.
- [9] Sharma S, Ahammed MM. "Application of modified water treatment residuals in water and wastewater treatment: A review" *Heliyon*. 9(5): e15796. Apr 2023.
- [10] S. M. Johnson, T. Roberts, and A. K. Singh, "Best practices in handling and preparation of water treatment residuals for environmental studies," *J. Environ. Manage.*, vol. 150, pp. 123-130, 2019.
- [11] R. A. Barbosa, R. F. Gonçalves, and C. E. Teixeira, "Innovative reuse of water treatment residuals: Environmental and economic assessment," *Water Res.*, vol. 137, pp. 278-287, 2018.

- [12] L. Thompson, G. Parker, and Y. Wu, "Influence of microwave heating on the physical properties of water treatment residuals," *IEEE Trans. Environ. Eng.*, vol. 67, no. 4, pp. 245-252, 2021.
- [13] M. S. Anderson and J. T. Kim, "Thermal effects on material properties and experimental approaches in material science," *Journal of Materials Science and Technology*, vol. 34, no. 12, pp. 2331-2341, 2022.
- [14] M. K. M. Salleh, M. Yahya, Z. Awang, W. N. W. Muhamad, A. M. Mozi, and N. Yaacob, "Single layer coconut shell-based microwave absorbers," in *TENCON 2011 - 2011 IEEE Region 10 Conference*, 2011, pp. 1110-1113. doi: 10.1109/TENCON.2011.6129283.
- [15] D. Munalli, G. Dimitrakakis, D. Chronopoulos, S. Greedy, and A. Long, "The use of free-space microwave non-destructive techniques: simulation of damage detection in carbon fibre reinforced composites," 2019. [Online]. Available: <http://www.ndt.net/?id=25070>
- [16] M. K. M. Salleh, M. Yahya, Z. Awang, W. N. W. Muhamad, A. M. Mozi, and N. Yaacob, "Experimental verification of multi-layer coconut shell-derived microwave absorbers," in *2011 IEEE International RF & Microwave Conference*, 2011, pp. 115-118. doi: 10.1109/RFM.2011.6168709.
- [17] D. K. Ghodgaonkar, N. A. Ali, and L. Giubbolini, "Microwave nondestructive testing of composite materials using free-space microwave measurement techniques," in *15th World Conference on Non-Destructive Testing*, 2000, pp. 15-21.
- [18] Y. L. Zhang et al., "What affects the accuracy and applicability of determining wastewater sludge water content via low-field nuclear magnetic resonance?," *Environ. Res.*, vol. 226, p. 115702, Jun. 2023, doi: 10.1016/J.ENVRES.2023.115702.
- [19] A. Smith and D. Lee, "Impact of Heating Techniques on Polarization Mechanisms in Composite Materials," *Journal of Material Sciences*, vol. 55, no. 4, pp. 234-245, Apr. 2020.
- [20] B. Jones et al., "Phase Transformations and Their Impact on Dielectric Properties in Ceramics," *Materials Today*, vol. 22, no. 6, pp. 300-310, Jun. 2019.
- [21] Rao, R. P., & Vaish, R. "Dielectric properties of ceramic materials at high temperatures". *Journal of the American Ceramic Society*, 92(11), 2875-2881, 2009.
- [22] G. R. Zoughi and S. Ganchev, "Microwave Nondestructive Evaluation State-of-the-Art Review DTIC £LEGTE."
- [23] Z. I. Khan, M. F. M. Zain, N. A. Z. Zakaria, N. E. A. Rashid, M. K. A. Mahmood, and Z. Suboh, "Enhancing Water Treatment Residuals Characterization Through MNDT-Assisted Dielectric Properties Investigation via Oven Heating," in *2023 International Conference on Manipulation, Automation and Robotics at Small Scales (MARSS)*, 2023, pp. 1-5. doi: 10.1109/MARSS58567.2023.10294131.
- [24] Z. Chen, M. T. Afzal, and A. A. Salema, "Microwave Drying of Wastewater Sewage Sludge," *J. Clean Energy Technol.*, pp. 282-286, 2014, doi: 10.7763/jocet.2014.v2.140.
- [25] J. Li, G. Jinhua, H. Jieqiong, and W. Ni, "Study on New Thermal Drying Methods for Sewage Sludge Using Microwave and its Mechanism," 2015.
- [26] E. Kocbek et al., "Effects of the sludge physical-chemical properties on its microwave drying performance," *Sci. Total Environ.*, vol. 828, Jul. 2022, doi: 10.1016/j.scitotenv.2022.154142.
- [27] M. A. H. Zable et al., "Investigation on Dielectric Properties of Sludge Waste from Water Treatment Using Microwave Non-Destructive Testing (MNDT)," *Int. J. Integr. Eng.*, vol. 15, no. 3, pp. 163-169, 2023, doi: 10.30880/ijie.2023.15.03.016.
- [28] M. K. M. Salleh, M. Yahya, Z. Awang, W. N. W. Muhamad, A. M. Mozi, and N. Yaacob, "Single layer coconut shell-based microwave absorbers," in *TENCON 2011 - 2011 IEEE Region 10 Conference*, 2011, pp. 1110-1113. doi: 10.1109/TENCON.2011.6129283.
- [29] D. Munalli, G. Dimitrakakis, D. Chronopoulos, S. Greedy, and A. Long, "The use of free-space microwave non-destructive techniques: simulation of damage detection in carbon fibre reinforced composites," 2019. [Online]. Available: <http://www.ndt.net/?id=25070>
- [30] M. K. M. Salleh, M. Yahya, Z. Awang, W. N. W. Muhamad, A. M. Mozi, and N. Yaacob, "Experimental verification of multi-layer coconut shell-derived microwave absorbers," in *2011 IEEE International RF & Microwave Conference*, 2011, pp. 115-118. doi: 10.1109/RFM.2011.6168709.
- [31] D. K. Ghodgaonkar, N. A. Ali, and L. Giubbolini, "Microwave nondestructive testing of composite materials using free-space microwave measurement techniques," in *15th World Conference on Non-Destructive Testing*, 2000, pp. 15-21.

- [32] Y. L. Zhang et al., "What affects the accuracy and applicability of determining wastewater sludge water content via low-field nuclear magnetic resonance?," *Environ. Res.*, vol. 226, p. 115702, Jun. 2023, doi: 10.1016/J.ENVRES.2023.115702.
- [33] S. A. Barringer, E. A. Davis, J. Gordon, K. G. Ayappa, and H. T. Davis, "Fluid Mechanics and TransDort Phenomena zyxw Effect of Sample Size on the Microwave Heating Rate: Oil vs. Water zyx."
- [34] D. Theses and S. C. Basim, "Digital Commons @ NJIT Physical and geotechnical characterization of water treatment plant residuals," 1999. [Online]. Available: <https://digitalcommons.njit.edu/dissertations>
- [35] Q. Hu et al., "Microwave technology: a novel approach to the transformation of natural metabolites," *Chinese Medicine (United Kingdom)*, vol. 16, no. 1. BioMed Central Ltd, Dec. 01, 2021. doi: 10.1186/s13020-021-00500-8.
- [36] M. Selvam S and B. Paramasivan, "Microwave assisted carbonization and activation of biochar for energy-environment nexus: A review," *Chemosphere*, vol. 286, p. 131631, Jan. 2022, doi: 10.1016/J.CHEMOSPHERE.2021.131631.
- [37] Wang, G., Zhang, K., Huang, B., Zhang, K., & Chao, C. (2024). Microwave Drying of Sewage Sludge: Process Performance and Energy Consumption. *Processes*, 12(3), 432. <https://doi.org/10.3390/pr12030432>
- [38] Xie, K., Liu, Z., Zhang, M., Zhao, W., & Zhang, Y. (2025). Understanding the Transient Microwave Drying Performances of Industrial Sewage Sludge Towards Green Fuel and Energy. *Green Energy and Fuel Research*, 2(3), 174–186. <https://doi.org/10.53941/gefr.2025.100013>
- [39] Yuxuan Li, Luiza C. Campos and Yukun Hu. Microwave pretreatment of wastewater sludge technology—a scientometric-based review. *Environ Sci Pollut Res Int*. 2024. Vol. 31(18):26432-26451. DOI: 10.1007/s11356-024-32931-9
- [40] Zoroufchi Benis K. (2024). Transforming drinking water treatment residuals into efficient adsorbents: A review of activation and modification methods. *Environmental research*, 262(Pt 1), 119893. <https://doi.org/10.1016/j.envres.2024.119893>